



Magnetic Resonance Imaging (MRI) Features and Diagnostic Accuracy in Pediatric Brachial Plexus Neuropathy: A Retrospective Analysis

Lili Zang¹, Xiaomin Duan^{2,*}, Xiaoyan Zhang¹, Jiexin Zhang¹, Jie Wang¹, Tong Yu², Guangheng Yin²

¹ Department of Radiology, Baoding Hospital, Beijing Children's Hospital Affiliated to Capital Medical University, Baoding, Hebei, China

² Imaging Center, National Center for Children's Health, Beijing Children's Hospital, Capital Medical University, Beijing, China

*Corresponding Author: Imaging Center, National Center for Children's Health, Beijing Children's Hospital, Capital Medical University, Beijing, China. Email: duanxiaomin0727@126.com

Received: 1 August, 2024; Revised: 5 December, 2024; Accepted: 13 December, 2024

Abstract

Background: Brachial plexus neuropathy is a common and frequently occurring disease that may present with upper limb numbness and dysfunction, leading to a high disability rate.

Objectives: To analyze the magnetic resonance imaging (MRI) features of brachial plexus neuropathy in children.

Methods: This study included 60 children who underwent MRI of the brachial plexus at our hospital from July 2019 to May 2024. The MRI scans included axial T₁WI and T₂WI sequences, axial and coronal T₂-STIR sequences, and coronal 3D-FIESTA sequences. The imaging results were analyzed to identify features of brachial plexus neuropathy.

Results: In this study, all 60 children underwent MRI of the brachial plexus. It was found that 34 (56.67%) cases were diagnosed as brachial plexus nerve injury via imaging, including 12 (20.00%) cases on the left side, 18 (30.00%) cases on the right side, and 4 (6.67%) cases on both sides. The imaging diagnoses were consistent with the clinical diagnoses in 32 cases and inconsistent in 2 cases. Meanwhile, 4 (6.67%) cases were diagnosed as other types of brachial plexus neuropathy, including 1 (1.67%) case of neurofibroma, 2 (3.33%) cases of neurosheathoma on the left side, and 1 (1.67%) case of right radicular sleeve cyst. The results were consistent with the clinical diagnoses in 3 cases and inconsistent in 1 case. Additionally, 7 (11.67%) cases were diagnosed as non-brachial plexus neuropathy, while 15 (25.00%) cases showed no obvious abnormality of the brachial plexus nerve. The sensitivity, specificity, and positive/negative predictive values were 100.00% (14/14), 78.95% (15/19), 91.11% (41/45), and 100.00% (15/15), respectively. The imaging features of brachial plexus nerve injury included thickening and thinning of nerve roots, high signals on T₂ fat-suppression sequences, small cystic low signals at the level of the intervertebral foramen, cystic dilatation of nerve roots, formation of spinal cysts, and irregularly shaped long T₁ and T₂ signals at the C₆ intervertebral foramen. The imaging features of neurofibroma included spike-shaped isometric T₁ and T₂ signals in the cervical soft tissues and high signals on T₂ fat-suppression sequences, with relatively homogeneous signals, a clear boundary, and an irregular morphology of the lesion wrapping around the brachial plexus nerve. Additionally, the imaging features of neurosheathoma included space-occupying lesions, predominantly oval-shaped isometric T₁ and slightly longer T₂ signals, located at the lateral upper edge of the thorax, the lower part of the posterior clavicle, and the left side of the brachial plexus.

Conclusions: The MRI can effectively show the location, range, and type of lesions, providing a valuable imaging reference for the early diagnosis and treatment of brachial plexus neuropathy in children.

Keywords: Brachial Plexus Neuropathy, Brachial Plexus Injury, Children, Magnetic Resonance Imaging

1. Background

Brachial plexus neuropathy is a common and frequently occurring disease that may present with upper limb numbness and dysfunction, leading to a

high disability rate (1, 2). More importantly, due to the complex anatomical structure of the brachial plexus, the formulation of clinical therapeutic plans depends primarily on determining the location and severity of lesions through imaging (3). Children are a high-risk group for brachial plexus neuropathy, with a worldwide

incidence rate of 0.38% - 5.10%; however, no relevant statistics are available for China (4).

Brachial plexus neuropathy in children includes neonatal brachial plexus injury caused by traction on the fetal shoulder and neck during delivery, as well as brachial plexus injury and neurogenic tumors resulting from trauma, autoimmune factors, and other causes. Different types of lesions require distinct treatments. Therefore, accurately determining the type, location, and severity of lesions using effective diagnostic methods is essential for developing early therapeutic plans and improving the cure rate.

Currently, the diagnosis of brachial plexus injury in clinical practice mainly relies on electromyography and neurological function tests. However, the probability of misdiagnosis and missed diagnosis remains high. Although spinal cord imaging via CT can identify brachial plexus injury, it primarily provides indirect signs and offers limited information, as it cannot visualize nerves outside the spinal canal. Thus, it presents certain limitations in clinical practice (5, 6).

Magnetic resonance imaging (MRI) offers significant advantages, including high-resolution imaging of soft tissues and multi-directional visualization, enabling clear display of the anterior and posterior parts of the brachial plexus nerve within the spinal canal (7). Recently, MRI has become the preferred auxiliary method for the clinical diagnosis of brachial plexus neuropathy. However, research on the diagnostic value of MRI for brachial plexus neuropathy has primarily focused on adult patients (8).

There are notable physiological differences between children and adults. Children have higher water content, lower fat content, smaller brachial plexus nerve trunks, and less distinct tissue and organ boundaries, which can limit the application of MRI in evaluating the brachial plexus nerve in this group.

2. Objectives

This study aims to analyze the MRI results of pediatric brachial plexus neuropathy, observe the imaging manifestations in affected children, and address the clinical research gap regarding MRI diagnosis of pediatric brachial plexus neuropathy.

3. Methodology

3.1. General Information

The study included 60 children who underwent MRI of the brachial plexus in our hospital from July 2019 to May 2024. The participants comprised 32 boys and 28

girls, aged between 17 hours and 14 years, with a median age of 15.5 months. Among them, 45 cases underwent MRI plain scans, while 15 cases underwent both MRI plain and enhanced scans.

3.2. Inclusion Criteria

- Children presenting with unilateral or bilateral limb movement disorders at admission
- Children suspected of having brachial plexus neuropathy
- Children aged ≤ 14 years
- Guardians of the children who were informed of the research content and provided signed informed consent

3.3. Exclusion Criteria

- Children with traumatic brain injury or neck deformities
- Children with implanted pacemakers, joint prostheses, metal dentures, etc.
- Children with a history of brachial plexus nerve conditions

Before undergoing MRI, the guardians were informed of all relevant details, including precautions for the examination, and signed informed consent forms. All children underwent electromyography to confirm the presence of brachial plexus injury. This study was reviewed and approved by the Medical Ethics Committee (No.: QFYLL2018010; Date: March 18, 2024), and no ethical or moral hazards were identified (9). After the MRI examination, all study subjects also underwent electrophysiological examinations to determine the presence of brachial plexus nerve injury.

3.4. Methods

Preparation for examination: Sleep deprivation was used for children who could not cooperate with the examination. Chloral hydrate was administered at a dose of 50 mg/kg, either orally or by enema, for sedation. Alternatively, comfort nursing was provided for MRI. During the scan, children were positioned supine, with towel pads used to properly wrap and fix their heads and shoulders. A 16-channel head/neck coil was employed, with the scanning range extending from C₁ to T₁₁, covering both bilateral shoulder joints.

Equipment: The MRI system used was the GE Signa 1.5T (GE, USA), along with a 16-channel head/neck coil (coil length: 26 cm).

3.4.1. Parameters

- Axial T₁WI and T₂WI sequences: Layer thickness of 3.0 mm, layer spacing of 0 mm, scan matrix of 256 × 224, field of view of 20 cm × 20 cm, average number of acquisitions (n=1), and number of excitations (n=4);

- Axial and coronal T₂-STIR sequences: TR of 4546 ms, TE of 42 ms, echo train length of 16, matrix of 256 × 192, layer thickness of 3.0 mm, layer spacing of 0 mm, field of view of 20 cm × 20 cm, average number of acquisitions (n=1), and number of excitations (n=4);

- Coronal 3D-FIESTA sequences: TR of 5.5 ms, TE of 2.0 ms, flip angle of 65°, matrix of 256 × 256, field of view of 20 cm × 20 cm, average number of acquisitions (n=1), and number of excitations (n=4).

3.5. Image Post-processing

The acquired images were transmitted through the intra-hospital network system to the Picture Archiving and Communication System. Two radiologists with ≥ 5 years of MR diagnostic experience independently observed and analyzed the MRI images in a double-blind manner. In cases of disagreement, the final result was determined through consultation. Finally, the head of the imaging department conducted a final review of the imaging results.

3.6. Signs of Brachial Plexus Neuropathy on Magnetic Resonance Imaging

Brachial plexus injury signs on MRI:

3.6.1. Direct Signs

3.6.1.1. Preganglionic Injury

Discontinuity or loss of continuity between the anterior and posterior intra-spinal nerve roots, thickening, stiffness, and tortuosity of the anterior and posterior nerve roots that cannot be traced continuously to the intervertebral foramen, discontinuity or loss of continuity of the anterior and posterior nerve roots, or a significant reduction in the number of anterior and posterior nerve roots on the coronal plane compared to the contralateral side.

3.6.1.2. Postganglionic Injury

Local accumulation of cerebrospinal fluid within the spinal canal, traumatic spinal cysts in the intervertebral foramen, or abnormal and asymmetrical morphology of the nerve root sleeve bilaterally.

3.6.2. Indirect Signs

Disappearance of nerve bundle structures, swelling, thickening, and deformation of nerve roots and trunks, rigid distribution, and high signal intensities on T₂WI and T₂-STIR sequences (Figure 1).

4. Results

4.1. Diagnostic Results of Brachial Plexus via Magnetic Resonance Imaging Examination

In this study, 60 children underwent MRI of the brachial plexus. Thirty-four cases were diagnosed with brachial plexus nerve injury, including 12 cases on the left side, 18 cases on the right side, and 4 cases on both sides. These MRI diagnoses were consistent with the clinical diagnoses in 32 cases and inconsistent in 2 cases. Among the two inconsistent cases, one diagnosed with right brachial plexus nerve injury was clinically confirmed as chronic inflammatory demyelinating polyradiculoneuropathy (CIDP), while the other, diagnosed with bilateral brachial plexus nerve injury, was clinically diagnosed with peripheral neuropathy.

Meanwhile, 4 cases were diagnosed with other types of brachial plexus neuropathy, including 1 case of neurofibroma, 2 cases of neurosheathoma on the left side, and 1 case of a right radicular sleeve cyst. These diagnoses were consistent with the clinical diagnoses in 3 cases and inconsistent in 1 case. The case of the right radicular sleeve cyst diagnosed via imaging was clinically confirmed as acute disseminated encephalomyelitis.

Seven cases were diagnosed as non-brachial plexus neuropathy through imaging, including 1 case of shoulder injury, 1 case of neck injury, 1 case of right clavicle fracture, 3 cases of cervical mass, and 1 case of lymphangioma. The imaging diagnoses were consistent with the clinical diagnoses in 6 cases and inconsistent in 1 case. One case, diagnosed with a right clavicle fracture on imaging, was clinically confirmed to have encephalopathy.

In addition, 15 cases showed no obvious abnormality of the brachial plexus nerve. The sensitivity, specificity, and positive/negative predictive values were 100.00% (14/14), 78.95% (15/19), 91.11% (41/45), and 100.00% (15/15), as shown in Tables 1 and 2.

4.2. Magnetic Resonance Imaging Features of Brachial Plexus Neuropathy

Among the 32 cases clinically diagnosed with brachial plexus nerve injury, the imaging features included thickening of the nerve roots, which were observed in the following distributions: C₄ ~ C₅ in 1 case,

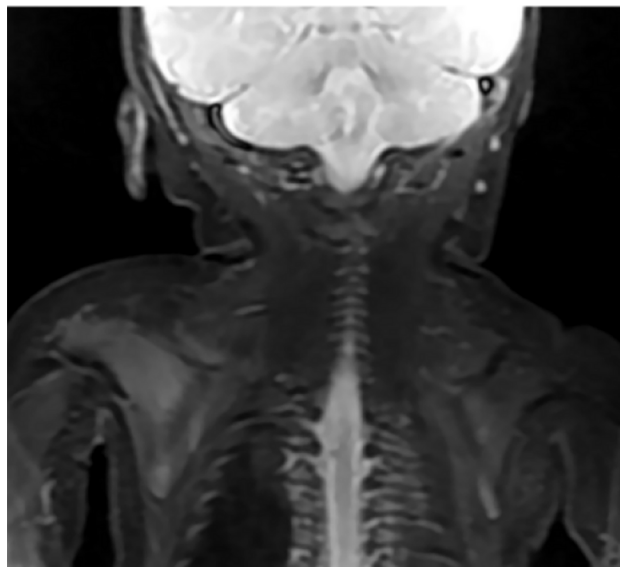


Figure 1. Indirect signs of brachial plexus injury on magnetic resonance imaging (MRI), a 20-day-old female infant with right upper limb movement disorder after birth, showing denervation changes in the muscles innervated by the brachial plexus as indicated by imaging (T_2 -STIR on the coronal plane), with high signals observed on T_2 -weighted MRI in the shoulder girdle muscle group.

Table 1. Magnetic Resonance Imaging and Clinical Results of Brachial Plexus Nerves in 60 Pediatric Patients

Relationship with Clinical Diagnosis	Brachial Plexus Injury	Other Brachial Plexus Neuropathy	Non Brachial Plexus Neuropathy	Normal Brachial Plexus Nerve
Matched	32 (53.33)	3 (5.00)	6 (10.00)	15 (25.00)
Not matched	2 (3.33)	1 (1.67)	1 (1.67)	0 (0.00)

$C_4 \sim C_6$ in 1 case, C_5 in 1 case, $C_5 \sim C_7$ in 10 cases, $C_5 \sim C_8$ in 2 cases, $C_5 \sim T_1$ in 10 cases, C_6 in 2 cases, $C_6 \sim C_8$ in 3 cases, $C_6 \sim T_1$ in 1 case, and C_7 in 1 case. Thinning of nerve roots was seen in 2 cases, specifically at $C_6 \sim C_7$ in 1 case and $C_7 \sim C_8$ in 1 case. Tortuosity of the brachial plexus nerve root was observed in 3 cases involving $C_5 \sim T_1$ and in 1 case involving $C_6 \sim C_7$. Additionally, 17 cases showed high signals on the T_2 fat-suppression sequence, 1 case exhibited long T_2 signals, and 1 case showed high signals on the STIR fat-suppression sequence (Figure 2A).

Other imaging features included small cystic low signals at the $C_7 \sim C_8$ intervertebral foramen, cystic dilatation of nerve roots (Figure 2B), formation of spinal cysts at $C_5 \sim T_1$ (Figure 2C), and irregularly shaped long T_1 and T_2 signals at the C_6 intervertebral foramen.

In the remaining 2 cases, where the imaging did not meet the clinical diagnosis, the following features were noted:

- In one case, the imaging revealed slight thickening of the C_5 brachial plexus nerve on the right side compared to the contralateral side, with symmetrical enhancement of the intra-spinal nerve root on contrast-enhanced scanning. The roots and trunks of the remaining bilateral brachial plexus nerves ($C_6 \sim T_1$) displayed normal distribution with uniform signals and no obvious abnormalities. No abnormal signals were found in the surrounding soft tissues, and the middle and distal segments of the brachial plexus nerve were poorly displayed. The final clinical diagnosis for this case was CIDP.

- In the other case, the imaging showed uneven thickening and enhancement of the right brachial plexus nerve, with slight uneven thickening and mild

Table 2. Magnetic Resonance Imaging Diagnosis of Brachial Plexus Neuropathy

MRI Scan	Clinical Diagnosis		Total
	Brachial Plexus Neuropathy	Non Brachial Plexus Neuropathy	
Brachial plexus neuropathy	41 (68.33)	0 (0.00)	41
Non brachial plexus neuropathy	4 (6.67)	15 (25.00)	19
Total	45	15	60

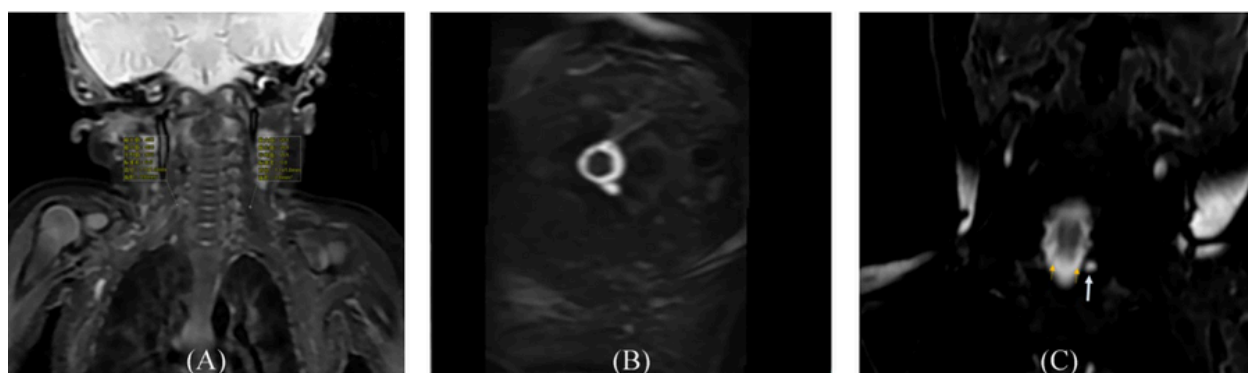


Figure 2. Magnetic resonance imaging (MRI) features of brachial plexus injury; A, the same infant as in Figure 1, showing imaging features of swelling and thickening of the right nerve root and trunk, as well as a stiff distribution and higher T_2 signal compared to the contralateral side; B, a 25-day-old male infant with left upper limb mobility disorder, showing the absence of the left nerve root, with corresponding nerve root sleeve dilation indicated by imaging (T_2 -STIR on the axial plane); C, the same infant as in Figure 1, showing the pre-ganglionic nerve root (thin arrow) on a coronal 3D-FIESTA sequence, with a linear equisignal nerve root on the right, disappearance of the left pre-ganglionic nerve root, and a small cystic lesion (long arrow) at the left margin, indicating a traumatic meningeal cyst.

enhancement of the left brachial plexus nerve. No obvious abnormal signals were detected in the surrounding soft tissues. Multiple enlarged lymph nodes were observed in the bilateral cervical regions, with the right lymph node having a long diameter of about 18.2 mm. The clinical diagnosis for this case was peripheral neuropathy.

The imaging features of 1 case clinically diagnosed with neurofibroma included pike-shaped isometric T_1 and T_2 signals in the cervical soft tissues (Figure 3A), along with high signals on the T_2 fat-suppression sequence. The lesion displayed relatively homogeneous signals, a clear boundary, and irregular morphology, surrounding the brachial plexus nerve. It extended up to the C_4 level and down to the cervical root, locally extending into the right $C_4 \sim C_5$ and $C_5 \sim C_6$ intervertebral foramina, with a close relationship to the adjacent vertebral arteries. The lesion showed significant and uniform enhancement on enhanced scanning (Figure 3B).

In contrast, the imaging features of 1 case diagnosed clinically as neurosheathoma included space-occupying

lesions predominantly characterized by oval-shaped isometric T_1 and slightly longer T_2 signals, located at the lateral upper edge of the left thorax, the lower part of the posterior clavicle, and the left side of the brachial plexus. These lesions exhibited uneven high signal intensity on the fat-suppression sequence, with the distal end slightly extending towards the axilla. Enhanced scanning revealed significant uneven enhancement of the lesion (Figure 3C), with a clear boundary between the lesion and the adjacent soft tissues. Additionally, in 1 case of neurosheathoma, the left $C_6 \sim C_8$ and T_1 brachial plexus nerves were thicker and more rigid compared to the contralateral side, with an unclear boundary from the lesion.

5. Discussion

The brachial plexus, composed of the cervical $C_5 \sim C_8$ and T_1 nerve roots, is a network of nerves that innervates the sensory and motor structures of the upper limbs, shoulders, back, and chest (10). Brachial plexus neuropathy can occur when the neural structures are subjected to excessive tension, compression, or

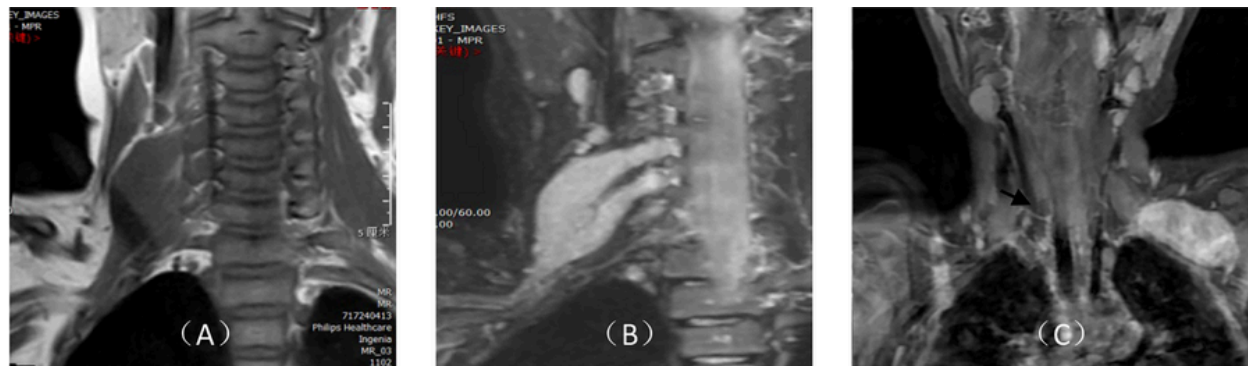


Figure 3. Magnetic resonance imaging (MRI) features of brachial plexus injury; A, a space-occupying lesion with pike-shaped isometric T₁ signals in the right cervical soft tissue, showing relatively uniform signals, a clear boundary, and irregular morphology wrapping around the right brachial plexus nerve; B, significant and uniform enhancement on enhanced scanning; C, oval-shaped space-occupying lesions in the lateral upper edge of the left thorax, the lower part of the posterior clavicle, and the left side of the brachial plexus, showing significant uneven enhancement on enhanced scanning.

traumatic injury. The brachial plexus is closely related to the median, radial, and ulnar nerves. Therefore, brachial plexus neuropathy can cause numbness and loss of sensation in the upper limbs, weakened muscle strength in the upper and middle parts of the latissimus dorsi and pectoralis major muscles, functional disorders in the elbow and wrist joints, and even complete paralysis of the upper limbs, which severely affects the normal life and quality of life of patients. It may also hinder the normal growth and development of children with brachial plexus injuries. While some children with brachial plexus injuries may recover spontaneously (11), others who do not recover or suffer from severe injuries may experience muscle and joint atrophy, and even lifelong disability, if not treated in a timely and effective manner (12). Therefore, accurately determining the type, location, and severity of the lesion using effective measures is of great significance for improving the prognostic outcome in affected children (13). Although ultrasound and electromyography can be used for diagnosing brachial plexus neuropathy, ultrasound accuracy is dependent on the examiner's skill and experience, making it slightly less reliable. Electromyography is an invasive procedure that is difficult to perform in children due to poor cooperation, limiting its clinical applicability. MRI is currently recognized as the most valuable and non-invasive imaging modality for diagnosing brachial plexus neuropathy (14, 15).

Children, especially newborns, have thin brachial plexus nerve trunks, with high water content and low fat content in the body. This poses a significant technical challenge for imaging the brachial plexus in children

using MRI. However, in some well-regarded domestic and international studies (16), high-resolution brachial plexus MRI has proven to be feasible for evaluating the physical connections between the brachial plexus and the spinal cord in children. As a result, MRI may hold decisive diagnostic value for brachial plexus neuropathy in children (17, 18).

According to previous studies (19), MRI of the brachial plexus in China is commonly performed in large 3A-grade hospitals using 3.0T MRI equipment, which provides a stronger magnetic field intensity for clearer and more accurate images. However, some researchers (20) have proposed that the uniformity of fat-suppression with 1.5T MRI is higher than that of 3.0T MRI, which helps avoid uneven fat-suppression in the brachial plexus nerve background under high field intensity. Therefore, this study employed 1.5T MRI to acquire high-quality images. The imaging findings in this study revealed that, among the 32 children clinically diagnosed with brachial plexus nerve injuries, MRI images showed thickening, thinning, tortuosity, or uneven thickness of nerve roots, accompanied by high signals in the T₂ fat-suppression sequence in some cases. These are generally considered signs of brachial plexus nerve injury. Additionally, MRI in another case revealed the formation of a meningeal cyst, indicating that the presence of a meningeal cyst does not necessarily imply nerve root discontinuity, which is consistent with previous research (21).

Furthermore, regarding the MRI features of neurofibroma, Li et al. (22) found that MRI images of neurofibroma showed uneven signals, with separated

short T₂ signal shadows, and plexiform neurofibromas with separation, which were similar to those observed in this study. Meanwhile, the imaging features of neurosheathoma included space-occupying lesions, predominantly oval-shaped with isometric T₁ and slightly longer T₂ signals, located in the lateral upper edge of the thorax, the lower part of the posterior clavicle, and the left side of the brachial plexus. In a prior study (23), its imaging features were generally summarized as a single oval mass with a clear boundary, a liquid echogenic zone in the tumor, or the "rat tail sign" at both ends, which were consistent with the pathological morphology observed in our study. However, the presence of the liquid echogenic zone was not found in the imaging diagnosis of this tumor in this study, which requires further confirmation. There is also a discrepancy between the MRI diagnosis and the clinical diagnosis in this study, which may be related to the different information and diagnostic perspectives obtained by the imaging and clinical physicians. More communication between the two is needed to reduce diagnostic discrepancies. The findings of this study can provide insights for the clinical diagnosis of pediatric brachial plexus neuropathy, enabling early and accurate diagnosis, which facilitates early treatment and maximizes patient recovery.

This study also has limitations, such as being a single-center retrospective analysis with a short follow-up period, which may limit its generalizability. It is recommended that future multi-center, large-scale observational studies be conducted to further clarify the impact of MRI on different types of brachial plexus neuropathy in children.

5.1. Conclusions

In conclusion, MRI offers advantages in clearly presenting the type, location, and extent of brachial plexus neuropathy in children, which is of great significance for the early diagnosis and treatment of this condition.

Footnotes

Authors' Contribution: Z. L. L. and D. X. M.: Designed the study; Z. X. Y. and Z. J. X.: Collected and analyzed the data; W. J., Y. T., and Y. Gh.: Wrote the manuscript. All authors have read and approved the final version of the manuscript.

Conflict of Interests Statement: The authors declared no conflicts of interest.

Data Availability: The dataset presented in the study is available on request from the corresponding author during submission or after publication.

Ethical Approval: The study was approved by the Institutional Ethics Committee of our Hospital (No.: QFYLL2018010; date: March 18, 2024).

Funding/Support: This study was supported by the Baoding Science and Technology Plan Project: Clinical study on the diagnostic effect of multimodal MR imaging technology in brachial plexus nerve injury in infants and young children (No.:2041F003).

Informed Consent: Written informed consent was obtained from all children and their parents.

References

- Gilcrease-Garcia BM, Deshmukh SD, Parsons MS. Anatomy, Imaging, and Pathologic Conditions of the Brachial Plexus. *Radiographic J*. 2020;**40**(6):1686-714. [PubMed ID: 33001787]. <https://doi.org/10.1148/rg.2020200012>.
- Portwood KE, Albayram MS, Stone S, Zingariello CD, Sladky JT, Chim H, et al. Clinical, electrophysiological, and imaging findings in childhood brachial plexus injury. *Dev Med Child Neurol*. 2022;**64**(10):1254-61. [PubMed ID: 35524644]. [PubMed Central ID: PMC9544348]. <https://doi.org/10.1111/dmcn.15255>.
- Koneru S, Nguyen VT, Hacquebord JH, Adler RS. Brachial Plexus Nerve Injuries and Disorders: MR Imaging-Ultrasound Correlation. *Magn Reson Imaging Clin N Am*. 2023;**31**(2):255-67. [PubMed ID: 37019549]. <https://doi.org/10.1016/j.mric.2023.01.006>.
- O'Berry P, Brown M, Phillips L, Evans SH. Obstetrical Brachial Plexus Palsy. *Curr Probl Pediatr Adolesc Health Care*. 2017;**47**(7):151-5. [PubMed ID: 28709767]. <https://doi.org/10.1016/j.cppeds.2017.06.003>.
- Girard AO, Suresh V, Lopez CD, Seal SM, Tuffaha SH, Redett RJ, et al. Radiographic imaging modalities for perinatal brachial plexus palsy: a systematic review. *Childs Nerv Syst*. 2022;**38**(7):1241-58. [PubMed ID: 35536348]. <https://doi.org/10.1007/s00381-022-05538-z>.
- Griffith JE. Ultrasound of the Brachial Plexus. *Semin Musculoskelet Radiol*. 2018;**22**(3):323-33. [PubMed ID: 29791960]. <https://doi.org/10.1055/s-0038-1645862>.
- Xiao R, Chen J, Zeng C, Feng X, Li T, Das SK, et al. Development of magnetic resonance imaging of brachial plexus neuralgia. *Neurol Sci*. 2022;**43**(3):1685-93. [PubMed ID: 35092542]. <https://doi.org/10.1007/s10072-022-05915-1>.
- Wade RG, Takwoingi Y, Wormald JCR, Ridgway JP, Tanner S, Rankine JJ, et al. Magnetic resonance imaging for detecting root avulsions in traumatic adult brachial plexus injuries: protocol for a systematic review of diagnostic accuracy. *Syst Rev*. 2018;**7**(1):76. [PubMed ID: 29778092]. [PubMed Central ID: PMC5960500]. <https://doi.org/10.1186/s13643-018-0737-2>.
- Shrestha B, Dunn L. The Declaration of Helsinki on Medical Research Involving Human Subjects: A Review of Seventh Revision. *J Nepal Health Res Counc*. 2020;**17**(4):548-52. [PubMed ID: 32001865]. <https://doi.org/10.33314/jnhrc.v17i4.1042>.
- Upadhyaya V, Upadhyaya DN, Mishra B. MR neurography in traumatic, non-obstetric paediatric brachial plexopathy. *Eur Radiol*. 2018;**28**(6):2417-24. [PubMed ID: 29318427]. <https://doi.org/10.1007/s00330-017-5217-x>.

11. Mazal AT, Faramarzalain A, Samet JD, Gill K, Cheng J, Chhabra A. MR neurography of the brachial plexus in adult and pediatric age groups: evolution, recent advances, and future directions. *Expert Rev Med Devices*. 2020;**17**(2):111-22. [PubMed ID: 31964194]. <https://doi.org/10.1080/17434440.2020.1719830>.
12. Bahm J. Looking through different lenses at neonatal brachial plexus injuries. *Dev Med Child Neurol*. 2022;**64**(10):1186-7. [PubMed ID: 35451053]. <https://doi.org/10.1111/dmcn.15250>.
13. Payen M, Didier M, Vialle R, Lehericy S, Fitoussi F, Bachy M. MRI of brachial plexus using diffusion tensor imaging: a pilot study for the use of resolve sequence surgical and radiologic anatomy. *Surg Radiol Anat*. 2023;**45**(12):1567-77. [PubMed ID: 37884742]. <https://doi.org/10.1007/s00276-023-03255-z>.
14. Koshinski JL, Russo SA, Zlotolow DA. Brachial Plexus Birth Injury: A Review of Neurology Literature Assessing Variability and Current Recommendations. *Pediatr Neurol*. 2022;**136**:35-42. [PubMed ID: 36084421]. <https://doi.org/10.1016/j.pediatrneurol.2022.07.009>.
15. Szaro P, McGrath A, Ciszek B, Geijer M. Magnetic resonance imaging of the brachial plexus. Part 1: Anatomical considerations, magnetic resonance techniques, and non-traumatic lesions. *Eur J Radiol Open*. 2022;**9**:100392. [PubMed ID: 34988263]. [PubMed Central ID: PMC8695258]. <https://doi.org/10.1016/j.ejro.2021.100392>.
16. Chuang CH, Huang CY, Ho SW, Chen CC. Rapid Detecting Brachial Plexus Injury by Point-of-Care Ultrasonography. *J Med Ultrasound*. 2022;**30**(4):303-5. [PubMed ID: 36844780]. [PubMed Central ID: PMC9944823]. https://doi.org/10.4103/jmu.jmu_185_21.
17. Menashe SJ, Ngo AV, Osorio MB, Iyer RS. Ultrasound assessment of glenohumeral dysplasia in infants. *Pediatr Radiol*. 2022;**52**(9):1648-57. [PubMed ID: 34549315]. <https://doi.org/10.1007/s00247-021-05180-y>.
18. Hardie C, Brooks J, Wade R, Teh I, Bourke G. Diagnostic accuracy of magnetic resonance imaging for nerve injury in obstetric brachial plexus injury: protocol for systematic review and meta-analysis. *Syst Rev*. 2022;**11**(1):173. [PubMed ID: 35987695]. [PubMed Central ID: PMC9392905]. <https://doi.org/10.1186/s13643-022-02037-9>.
19. Acharya AM, Cherian BS, Bhat AK. Diagnostic accuracy of MRI for traumatic adult brachial plexus injury: A comparison study with surgical findings. *J Orthop*. 2020;**17**:53-8. [PubMed ID: 31879474]. [PubMed Central ID: PMC6919346]. <https://doi.org/10.1016/j.jor.2019.08.015>.
20. Felisaz PF, Napolitano A, Terrani S, Parisi C, Toto-Brocchi M, Ce M, et al. An optimized 1.5 Tesla MRI protocol of the brachial plexus. *Neuroradiol J*. 2024;**37**(1):43-53. [PubMed ID: 37621183]. [PubMed Central ID: PMC10863567]. <https://doi.org/10.1177/19714009231196475>.
21. Lao Q, Jia Y, Zhao K, Liu K, Feng J. Value of High-Resolution MRI in the Diagnosis of Brachial Plexus Injury in Infants and Young Children. *Int J Gen Med*. 2022;**15**:5673-80. [PubMed ID: 35755861]. [PubMed Central ID: PMC9215839]. <https://doi.org/10.2147/IJGM.S362738>.
22. Li YZ, Liu YW, Wang SC, Tai J, Zhang J, Liu YH, et al. Clinical analysis of head and neck neurogenic tumor in childhood. *Lin Chuang Er Bi Yan Hou Tou Jing Wai Ke Za Zhi*. 2019;**33**(10). ZH. [PubMed ID: 31623049].
23. Vrinceanu D, Dumitru M, Popa-Cherecheanu M, Marinescu AN, Patrascu OM, Bobirca F. Extracranial Facial Nerve Schwannoma-Histological Surprise or Therapeutic Planning? *Medicina (Kaunas)*. 2023;**59**(6). [PubMed ID: 37374372]. [PubMed Central ID: PMC10302795]. <https://doi.org/10.3390/medicina59061167>.